

ELECTRONIC REJECTION OF OPTICAL CROSSTALK IN A TWIN PHOTOTUBE SCINTILLATION COUNTER

B. H. Laney

Nuclear-Chicago Corporation

Des Plaines, Illinois

ABSTRACT

Approximately 33% of the total background count rate of a conventional liquid scintillation counter is caused by optical crosstalk between the phototube detectors. These coincident events are produced by radioactive contamination and Cerenkov radiation in the phototube envelope — and by discharges within the tube structure. Over 75% of the crosstalk can be rejected by analyzing the relative pulse amplitude produced at each phototube output. The pulse amplitudes can be combined various ways to allow ordinary pulse height discriminators to separate crosstalk from legitimate events.

INTRODUCTION

Optical crosstalk is the coupling of light emanating from one phototube to the other.^{1,2} Light produced in one phototube and detected by the other will add to the coincidence background. The character of the light emitted depends upon the material and structure of the phototubes, the operating voltage, gain and amount of shielding. Efficient optical coupling between the sample and each phototube implies that the coupling between phototubes is efficient. Optical techniques to minimize the cross coupling such as masking, light traps, polarizers and filters, usually degrade figure of merit (E^2/B) as well as detection efficiency.

Optical crosstalk is defined as the empty chamber count rate less the accidental count rate. The accidental count rate ($2TN_1 N_2$) in modern scintillation systems is negligible i.e., below 0.5 counts per minute*, thus the optical crosstalk is essentially the empty chamber rate.

* The count rate obtained from a blackened vial may measure as high as 4 counts per minute resulting from light passing around the vial.

ANALYSIS OF BACKGROUND SPECTRA

The contribution of optical crosstalks to the summed background for a pair of EMI 9750 QB phototubes is shown in fig. 1. A single channel analyzer at tritium gain with dynamic range of 29 to 1 is used to gate the tritium spectrum shown in fig. 2. The ^{14}C spectrum is gated by a single channel analyzer, with a dynamic range of 8 to 1, set to include approximately 0.2% tritium. Since the upper discriminator of the ^3H channel is slightly below the lower discriminator of the dual label ^{14}C channel, the wide window ^{14}C background is only slightly greater than the sum of the two windows.

Two peaks are visible in the background spectrum of fig. 1. The lower energy peak is attributed to residual activity, particularly ^{40}K and ^{226}Ra in the glass ampoule. Replacing the glass ampoule with a nylon or polyethylene vial removes approximately 10 cpm. The upper energy peak is due to light emissions from the phototube as well as from scintillation produced in the liquid fluor by environmental radioactivity.

Coincident empty chamber spectra of 3 phototube types are shown in figs. 3, 4, and 5. Quartz and pyrex faced phototubes may be compared in figs. 3 and 5. The spectrum from a pair of RCA 4501 phototubes with CuBe first dynodes (not shown) measured the same as C31000C phototubes (fig. 4) with GaP first dynode. The crosstalk spectrum varies considerably in energy and intensity between pairs of the same tube, and dramatically between different tube types.

Most of the coincident empty chamber events of a pulse height less than 7 to 10 photoelectron equivalents (P.E.) are produced in the faceplate. Assuming that the ultraviolet transmission of the photocathode is less than 10%, it is highly improbable that a photon produced inside one phototube will be coincidentally detected by the other — unless many photons were spontaneously released. The scintillations in the faceplate are caused by residual activity in the faceplate and detector, and by Cerenkov radiation. Events at pulse heights greater than approximately 10 P.E. are principally produced by light emitted within the phototubes. Using 1 KeV per P.E., 10 P.E. corresponds to the lower half of the tritium spectrum. Although the count rates are comparable, the crosstalk in the RCA 8575 family is less than half the amplitude of the EMI two inch venetian blind structure (figs. 3, 4, and 5).

TWO PARAMETER PULSE HEIGHT ANALYSIS

Coincident pulse heights from scintillations produced within one tube tend to be unequal due to optical attenuation of the photocathode. The coincident empty chamber spectrum shown in fig. 8 depicts the pulse height from each phototube as independent X and Y variables along the abscissa and ordinate. The probability, $P \, dx \, dy$, is perpendicular to the page. Tritium (fig. 6) shows a poorer correlation between the X and Y pulse amplitudes than that of the ^{14}C spectrum (fig. 7) due to statistical variances produced by sample geometry and phototube resolution. The diagonal line through the spectra is a summed marker at 50% of range. One percent of the count rate is above full range.

ORGANIC SCINTILLATORS

The difference between summed and unsummed pulse height analysis is apparent from fig. 9, a and b. A summed tritium window excludes most of the crosstalk events from both tubes while an unsummed window includes the crosstalk from the gate tube. The opposite is true in the case of ^{14}C , which includes crosstalk from both tubes when summed, and excludes the crosstalk from the gate tube when unsummed.

If both inputs exceed a lower level (X "And" Y), rather than the sum, events along the axes can be rejected as shown in fig. 10a. The coincidence thresholds shown in fig. 9 are lower level "AND"s which, if increased above the crosstalk improves the ^{14}C figure merit with little loss in ^{14}C efficiency. However, tritium efficiency will be decreased using this technique. Conversely, greater crosstalk will become evident in systems yielding high tritium efficiency, whether due to lower quantum or to electronic thresholds. The lower level "AND" is not useful for a tritium or dual label ^{14}C window. The non-linear coincidence threshold (fig. 10b) is a more versatile version of the lower level "AND", because the coincidence threshold increases as a function of the pulse height from the opposite phototube. Though more difficult to implement, it does not compromise dual label separation.

When the coincidence resolving time is comparable to, or less than the rise time of the coincidence amplifier, a kind of crosstalk discrimination occurs. Unequal pulse heights from each phototube will reach threshold at different times. Small slow rising pulses reach threshold later and will be rejected in the presence of large fast rising events from the other phototube. The measured spectral shape of the thresholds, shown in figs. 6 and 7, is consistent with the theoretical shown in fig. 11.

The non-linear coincidence threshold can be approximated by adding a ratio or difference discriminator (fig. 12a and 12b) to the usual coincidence criteria. The difference discriminator (fig. 12b) generates the function by using sums and differences instead of ratios. The X and Y intercepts are set to exclude 0 to 1% of the tritium. The slope is set to reject 1 to 5% of the ^{14}C . The intercept and slope were determined empirically on the basis of maximizing E^2/B for tritium and ^{14}C respectively.

THE CROSSTALK DISCRIMINATOR

A block diagram (fig. 13) of the crosstalk discriminator (CTD) consists of four amplifiers and a pulse height discriminator. The first amplifier inverts -X to obtain a pulse amplitude equal to +X. The +X and -Y inputs are added together and amplified 150 times. Two diodes and a second inverter generate the absolute value of $150(X-Y)$. The last amplifier adds the inputs with the correct constants to obtain the function $75|X-Y|-4(X+Y)$ as a pulse height output. Output waveforms produced by ^{14}C and an empty chamber are shown in figs. 14 and 15 respectively. Pulses above the 60 millivolts discrimination level, D, initiate a digital output pulse. As shown in Fig. 16, the pulse inhibits the delayed

coincidence. The 200 ns calculation time of the CTD occurs during the 500 ns delay time. Since the circuit operates on X-Y at the outer edges of the spectrum (fig. 7), stability in excess of 0.2% of the count rate is easily maintained with ordinary metal film resistors and feedback amplifiers.

CONCLUSION

Performance of a typical Nuclear-Chicago Mark II TM liquid scintillation spectrometer with and without a CTD is shown in Table 1. The most significant improvement is in the ^{14}C window where 92% of the crosstalk has been eliminated reducing the background 45%. The ^{14}C figure of merit was increased from 340 to 610 without degrading the tritium efficiency or figure of merit. The stability of standards measured over a 22 day period was unaffected by the CTD i.e. one sigma measured less than 0.25%.*

ACKNOWLEDGMENT

The author thanks Dr. T.M. Kavanagh for discussions and experiments contributing to spectral analysis and acknowledges the assistance of H. Engberg who constructed and tested the experimental circuitry.

REFERENCES

1. H.R. Krall, "Extraneous Light Emission from Photomultipliers" IEEE Transactions on Nuclear Science NS14 No. 1, 1967.
2. G.A. Morton, H.M. Smith, R. Wasserman, "Afterpulses in Photomultipliers" IEEE Transaction on Nuclear Science, NS14 No. 1, 1967.
3. R.P. Randall, "Sources of Multi Electron Emissions in Very Low Dark Current Image Intensifiers" IEEE Transactions on Nuclear Science NS17 No. 3, 1970.

* Nuclear Chicago Model 8923 Auto-Calibration employed.

ORGANIC SCINTILLATORS

TABLE 1

EFFICIENCY AND BACKGROUND IN A TYPICAL MARK II LIQUID SCINTILLATION SPECTROMETER						
ENERGY RANGE	29:1 TRITIUM (³ H)		8:1 CARBON 14 (¹⁴ C)		TOTAL INTEGRAL	
	w/o CTD	with CTD	w/o CTD	with CTD	w/o CTD	with CTD
TRITIUM STANDARD % EFFICIENCY	64.5%	64.5%	0.19%	0.21%	65.3%	65.2%
CARBON 14 STANDARD % EFFICIENCY	18.5%	18.1%	74.7%	73.4%	98.1%	96.4%
BLANK STANDARD CPM	18.59	18.47	16.27	8.82	56.85	42.14
EMPTY CHAMBER CPM	3.02	2.26	13.42	1.00	19.09	3.47

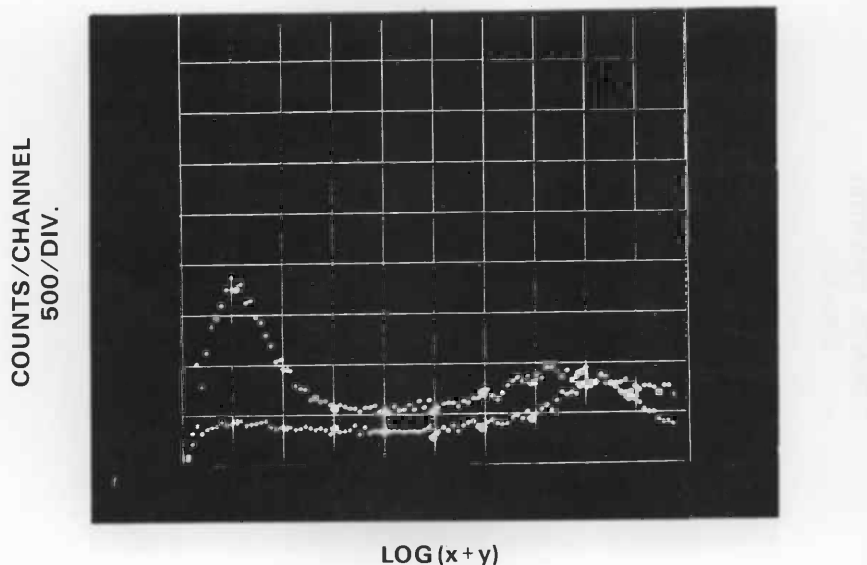


Fig. 1 — Pulse height spectra of a blank standard (upper) and an empty chamber (lower).

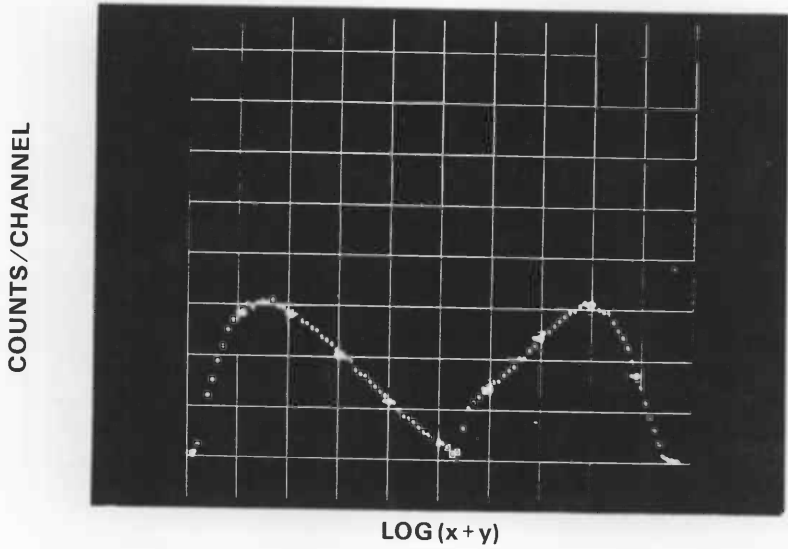


Fig. 2 — Pulse height spectra of tritium (left) and carbon 14 (right) gated by ^3H and ^{14}C ROI's.

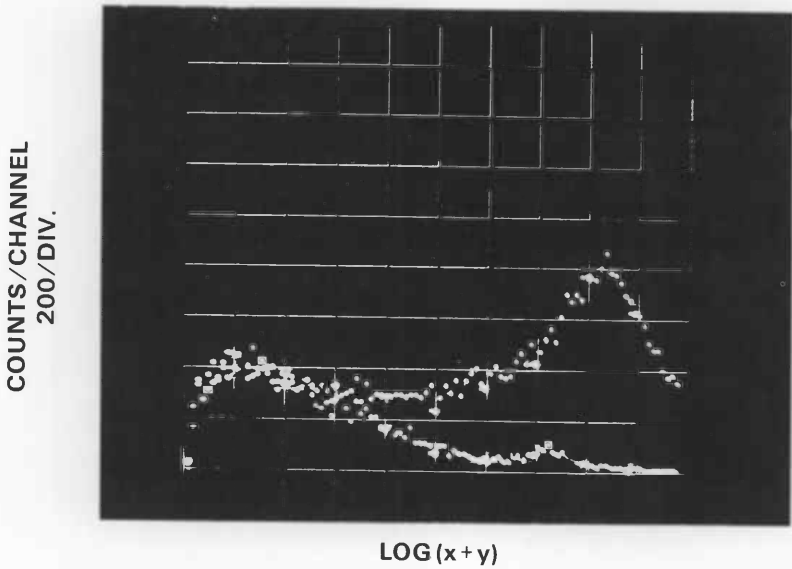
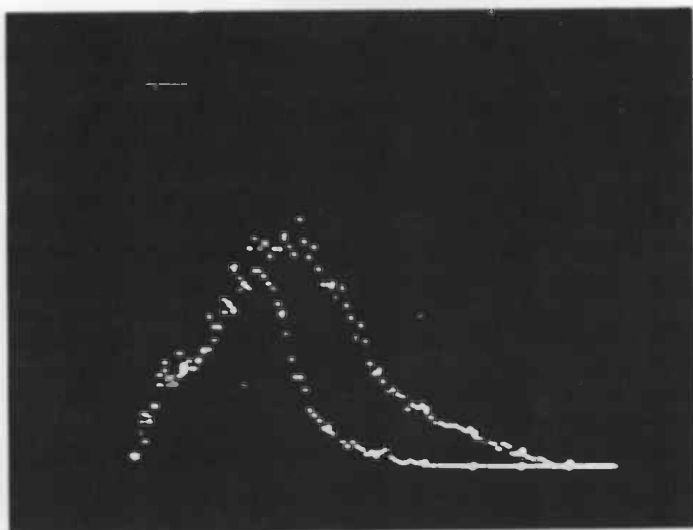


Fig. 3 — Pulse height spectra of an empty chamber from EMI 9750 QB photo-tubes: upper without CTD, lower with CTD.

ORGANIC SCINTILLATORS

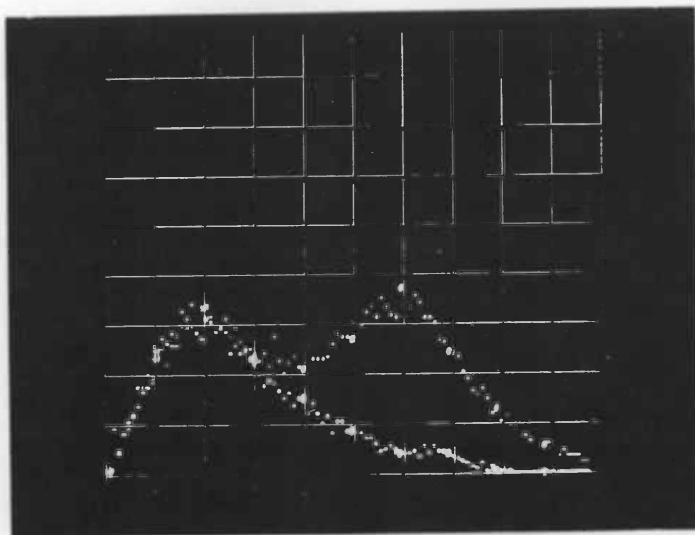
COUNTS/CHANNEL
200/DIV.



LOG(x+y)

Fig. 4 — Pulse height spectra of an empty chamber from RCA C31000C phototubes: upper without CTD, lower with CTD.

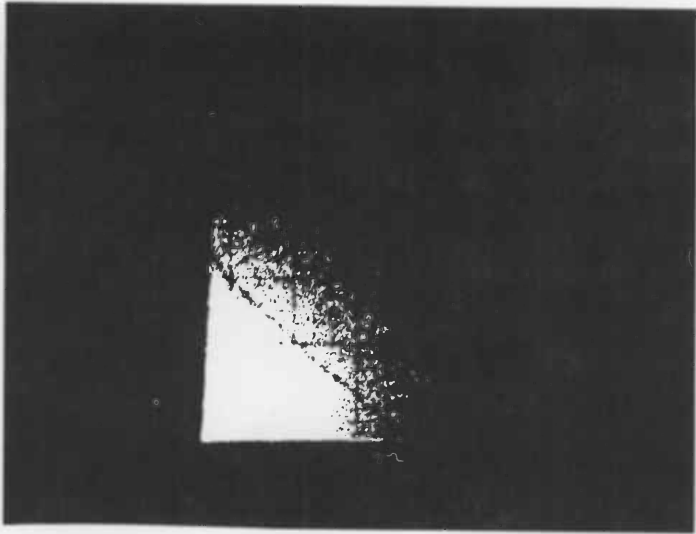
COUNTS/CHANNEL
200/DIV.



LOG(x+y)

Fig. 5 — Pulse height spectra of an empty chamber from EMI 9750B (pyrex) phototubes: upper without CTD, lower with CTD.

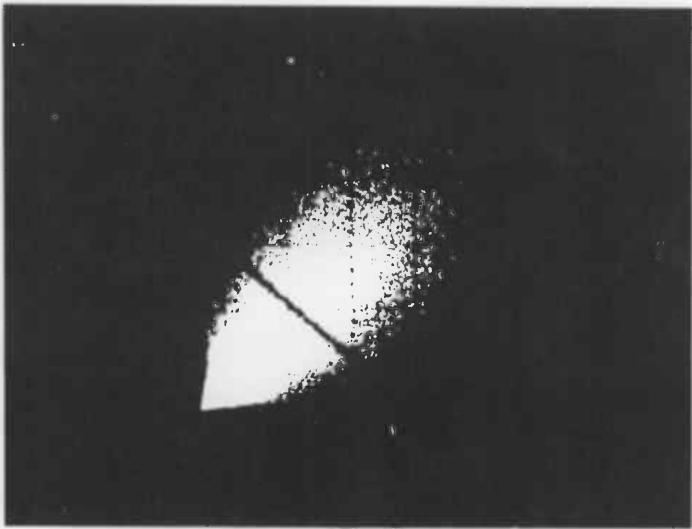
PULSE HEIGHT Y



PULSE HEIGHT X

Fig. 6 — Linear pulse height distribution of tritium at tritium attenuation.

PULSE HEIGHT Y

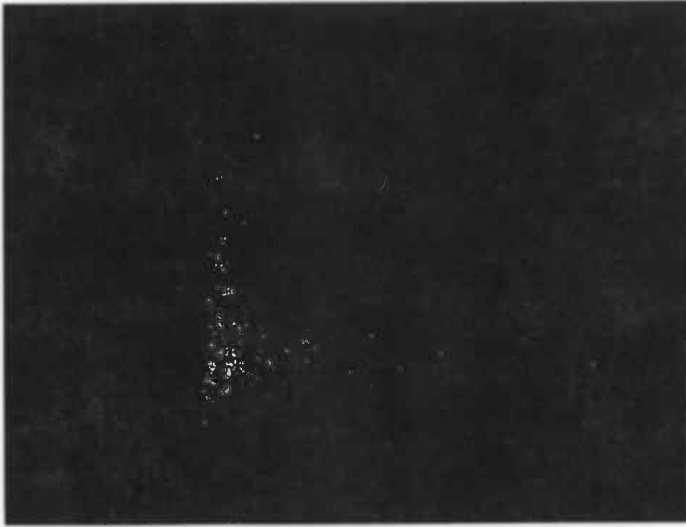


PULSE HEIGHT X

Fig. 7 — Linear pulse height distribution of carbon 14 at carbon 14 attenuation (8X tritium)

ORGANIC SCINTILLATORS

PULSE HEIGHT Y



PULSE HEIGHT X

Fig. 8 — Linear pulse height distribution of an empty chamber from EMI 9634QR phototubes at tritium attenuation.

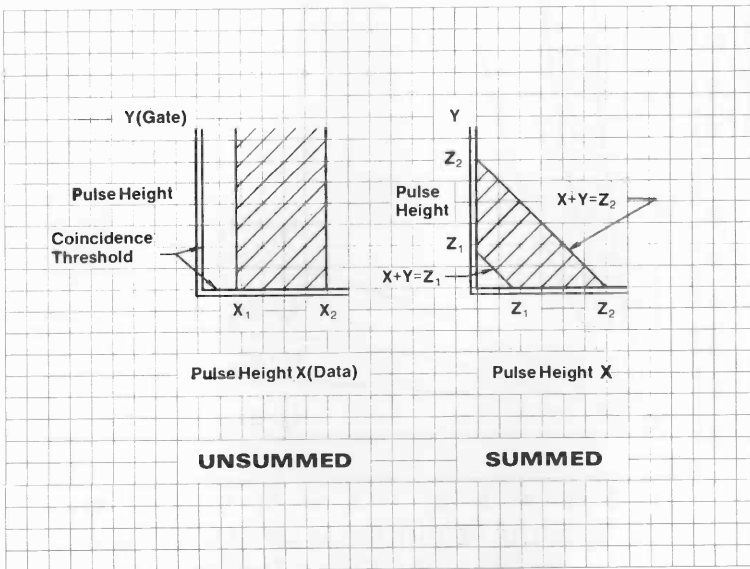


Fig. 9 — Comparison of unsunned and sunned pulse height analysis.

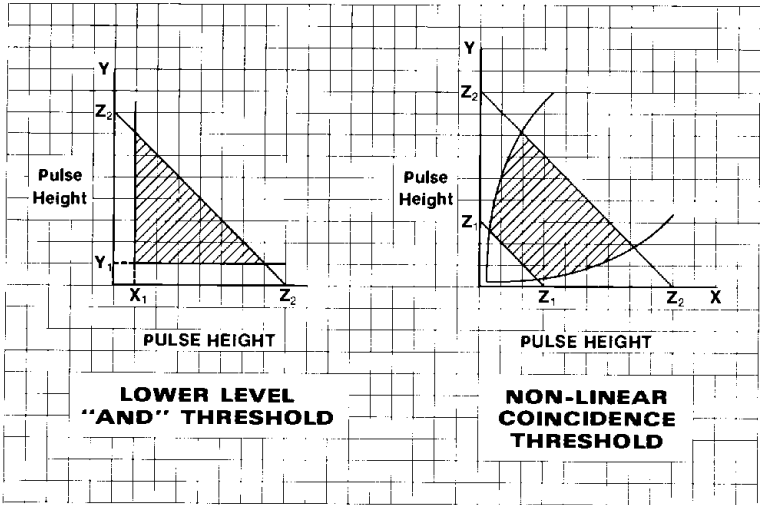


Fig. 10— Comparison of lower level "AND" and non-linear Coincidence Threshold

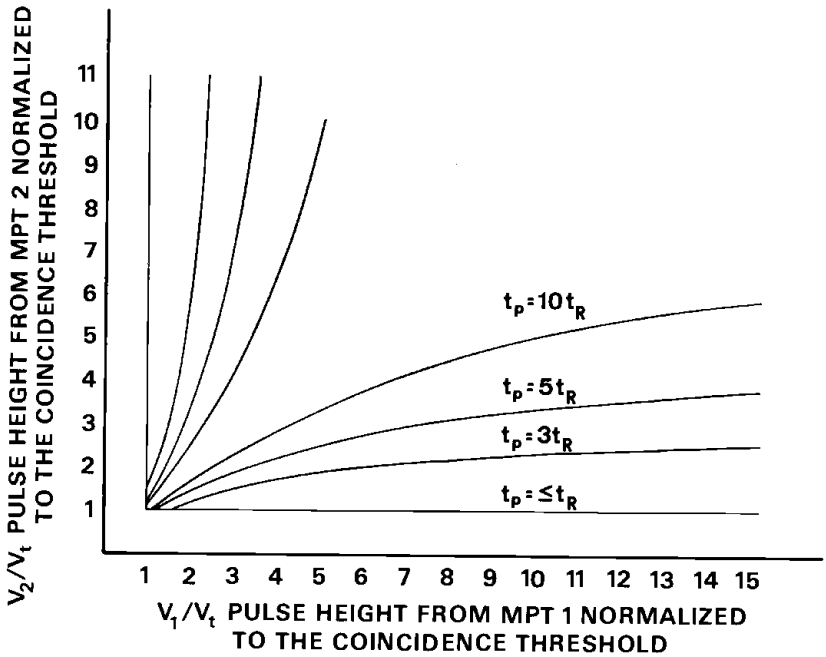


Fig. 11 — Theoretical Rise Time Effect on Coincident Threshold

ORGANIC SCINTILLATORS

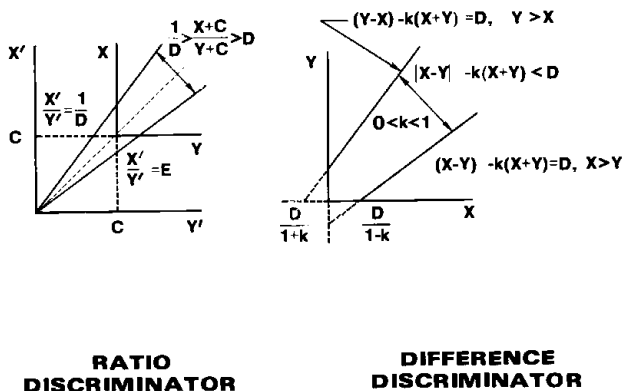


Fig. 12 — Comparison of Ratio to Difference Discriminator.

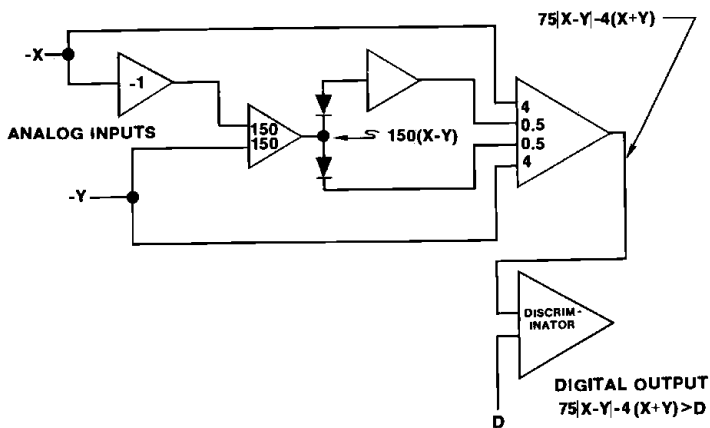
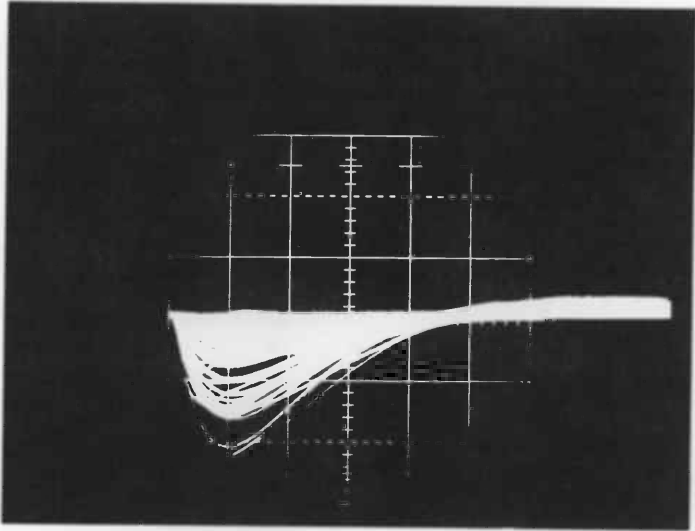


Fig. 13 — Cross Talk Discriminator

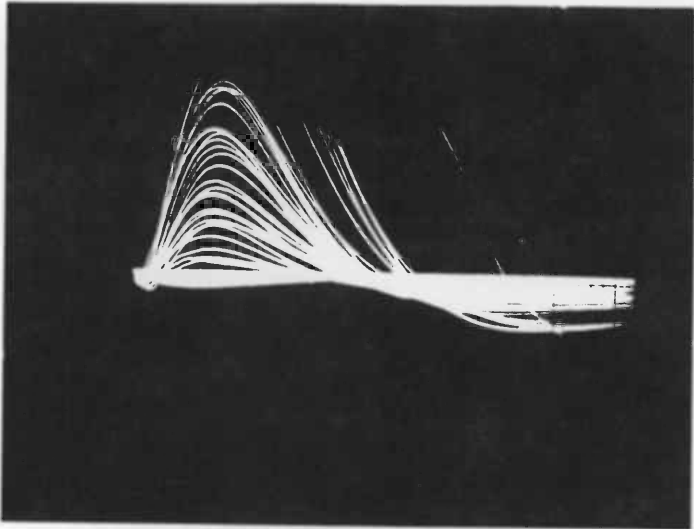
0.5V/DIV.



200 NS/DIV.

Fig. 14—CTD function output waveforms for carbon 14.

0.5V/DIV.



200 NS/DIV.

Fig. 15—CTD function output waveforms for an empty chamber.

ORGANIC SCINTILLATORS

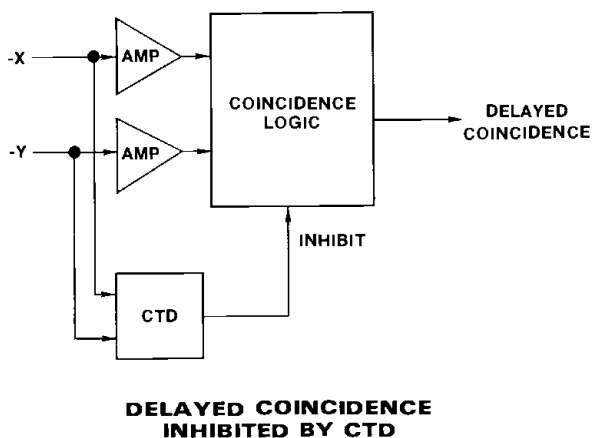


Fig. 16 — Delayed Coincidence Inhibited by CTD.

NOTES

All measurements were made on standard Nuclear-Chicago spectrometers with 180° opposed, air coupled phototubes, operated at approximately 50A/lumens with a high current voltage divider. The coincidence resolving time was approximately 30 nanoseconds followed by a 4 microsecond blanking interval to reject afterpulses. Live timing was employed for both coincident and non-coincident events.

The spectra shown in figs. 1, 2, 3, 4 and 5 were obtained from a Nuclear-Chicago Model 8928 multichannel analyzer interface module in the log mode. The compression tends to be linear for small pulse amplitudes.

Fig. 1, 2, 3, 14 and 15 were obtained from EMI 9750QB multiplier phototubes.

Fig. 6, 7 and 8 were obtained from EMI 9634QR multiplier phototubes.

Each spectrum shown in fig. 1, 3, 4 and 5 was accumulated for 1000 minutes at 100 channels full scale.